Chinese Chemical Letters 33 (2022) 541–546

Contents lists available at ScienceDirect

Chinese Chemical Letters

journal homepage: www.elsevier.com/locate/cclet

Highly selective and turn-on fluorescence probe with red shift emission for naked-eye detecting Al^{3+} and Ga^{3+} based on metal-organic framework

Linhui Wu[a], Shuli Yao[a], Hui Xu[a], Tengfei Zheng[a], Suijun Liu[a,*], Jinglin Chen[a], Na Li[b,*], Herui Wen[a]

[a] School of Chemistry and Chemical Engineering, Jiangxi University of Science and Technology, Ganzhou 341000, China
[b] School of Materials Science and Engineering, Tianjin Key Laboratory of Metal and Molecule-Based Material Chemistry, Nankai University, Tianjin 300350, China

ARTICLE INFO

Article history:
Received 29 April 2021
Revised 31 May 2021
Accepted 3 June 2021
Available online 12 June 2021

Keywords:
Metal-organic frameworks
Fluorescence probe
Naked-eye detection
Turn-on effect
Red shift emission
Al^{3+} and Ga^{3+}

ABSTRACT

A novel Zn^{II}-based metal-organic framework with the formula of $\{[Zn_2(BBIP)_2(NDC)_2]\cdot H_2O\}_n$ (**JXUST-5**) derived from 3,5-bis(benzimidazol-1-yl)pyridine (BBIP) and 1,4-naphthalenedicarboxylic acid (H_2NDC) has been synthesized. The adjacent Zn^{II} ions are linked through two BBIP ligands to form a $[Zn_2(BBIP)_2]$ secondary building unit (SBU). The neighbouring SBUs are further connected by NDC^{2-} with μ_2-η^1:η^1 and μ_2-η^1:η^1:η^1 bridging modes to form a two-dimensional (2D) framework. Topological analysis shows that **JXUST-5** could be simplified as an uninodal ***fes*** topology with a point symbol of $\{4.8^2\}$. Furthermore, the 2D framework net could be extended through C-H···π interaction to form the three-dimensional supramolecular structure. Luminescent experiments suggest that **JXUST-5** could selectively and sensitively recognize Al^{3+} and Ga^{3+} through fluorescence enhancement effect along with a relatively large red shift. The detection limits for Al^{3+} and Ga^{3+} are 0.17 and 0.69 ppm, respectively. Interestingly, the sensing process for both Al^{3+} and Ga^{3+} could be directly observed with naked eyes under 365 nm UV lamp. Notably, **JXUST-5** could be recycled at least five times as a fluorescent sensor toward Al^{3+} and Ga^{3+}, which is the second example of turn-on MOF based fluorescent sensor toward Ga^{3+}.

As the important metal elements, aluminum and gallium widely exist in the environment and in our daily [1,2], and they can enter the human body through food and drinking. However, excessive intake of Al^{3+} and Ga^{3+} can damage the immune system and endanger human health [3,4]. Hence, it is of crucial importance and attracts great attention to develop quick, efficient and reliable sensing materials for the detection of Al^{3+} and Ga^{3+} with high sensitivity and selectivity. Up to now, a series of luminescence probes have been reported for detecting Al^{3+} or Ga^{3+}. Gupta *et al.* reported a series of multiple hydroxyl–group-based fluorescence probes with turn-on effect toward Al^{3+} and Ga^{3+} [3]. A Co^{II}-based metal-organic framework (MOF) that can selectively detect Fe^{3+}, Cr^{3+} and Al^{3+} with fluorescence turn-on effect has been synthesized by our group [5]. Peng *et al.* designed a simple luminescent probe derived from 1,10-binaphthol for relay recognition of homocysteine and Group IIIA ions (Al^{3+}, Ga^{3+} and In^{3+}) [2].

As a class of emerging crystalline inorganic-organic hybrid materials, MOFs have received considerable attention from many chemists and material scientists for ever-expanding applications in gas storage and separation [6-8], catalysis [9-12], drug delivery [13-16], chemical sensing [17-24] and magnetism [25-27]. Additionally, these materials show high inherent porosity, structural diversity, and adjustable physicochemical properties. The unique advantages in terms of structural tailoring and performance modulation make MOF an ideal platform for the design of chemical sensors.

So far, the luminescent MOFs have been extensively explored as chemical probes for metal ions [28-32], small organic molecules [33-35], and nitroaromatic compounds [36,37]. Generally, the host-guest interactions between analytes and MOFs or energy transfer are the main reasons of luminescence quenching (turn-off) phenomena of MOF-based sensors. The turn-off sensing seriously limits the sensitivity and selectivity of MOF sensors for targeted analysts. Therefore, it is highly desirable to develop new MOF sensors based on luminescence turn-on effect for improving both the sensitivity and selectivity of MOF in chemical sensing applications.

* Corresponding authors.
E-mail addresses: sjliu@jxust.edu.cn (S. Liu), lina@nankai.edu.cn (N. Li).

https://doi.org/10.1016/j.cclet.2021.06.009
1001-8417/

Considering the structural and chemical variability nature of MOFs, a mixed-ligand assembly strategy based on the acid-base system [38-42] was chosen to construct the turn-on sensors. On account of the advantages of compensating charge balance, repulsive vacuum, coordination deficiency and weak interaction all at once, the acid-base mixed-ligand assembly strategy offers substantial opportunities for rationally designing and synthesizing MOFs materials with turn-on effect [43]. As a representative example, the bis(benzimidazole)-based ligands display excellent coordination abilities for the formation of MOFs with diverse structures and favorable properties [44]. As a semi-flexible N-rich pyridine- and benzimidazole-containing ligand, 3,5-bis(benzimidazol-1-yl)pyridine (BBIP) with pyridine groups offers potential interaction sites to react with analysts, which are advantageous for the sensing of metal ions due to the alterant electron or energy transfer process [45]. Additionally, a conjugated organic ligand with rich π electron and strong luminescence emission, 1,4-naphthalenedicarboxylic acid (H_2NDC), is adopted as an auxiliary ligand [46]. H_2NDC has been widely utilized to construct luminescent MOFs [47-49].

Herein, BBIP and H_2NDC are chosen as organic ligands (Scheme S1 in Supporting information) to design turn-on luminescent MOFs. To prepare desired luminescent MOFs, the suitable choice of metal ions is another important factor. It is well-known that Zn^{II} with d^{10} electron configuration was introduced into the mixed-ligand systems to construct the MOFs with excellent luminescence properties [50]. Therefore, a novel Zn^{II}-based luminescent MOF with the formula of $\{[Zn_2(BBIP)_2(NDC)_2]\cdot H_2O\}_n$ (**JXUST-5**) has been successfully synthesized and structurally characterized. Luminescent experiments demonstrate that **JXUST-5** could selectively and sensitively recognize Al^{3+} and Ga^{3+} through fluorescence enhancement effect with naked eyes along with a relatively large red shift. Notably, **JXUST-5** is the second case of turn-on MOF-based fluorescent sensor toward Ga^{3+} [51].

From the SEM image (Fig. 1a), the as-synthesized **JXUST-5** exhibits a blocky structure with an average particle size of 500 μm. The single crystal X-ray diffraction analysis shows that **JXUST-5** belongs to the space group $P2_1/c$ of monoclinic system, and the asymmetric unit is composed of two crystallographically independent Zn^{II} ions, two BBIP ligands, two NDC^{2-} ligands, and one free H_2O molecule. As shown in Fig. 1b, Zn1 shows a four-coordinated environment constructed with two O atoms (O1 and O5) from two distinct NDC^{2-} ligands and two N atoms (N5 and N10) from two different BBIP ligands, while Zn2 exhibits a five-coordinated environment established by three O atoms (O4A, O7B and O8B) from two distinct NDC^{2-} ligands and two N atoms (N1 and N6) from two different BBIP ligands. The Zn–O and Zn–N bond distances vary from 1.902(4) Å to 2.510(4) Å and 1.967(4) Å to 2.070(4) Å, respectively (Table S2 in Supporting information). Interestingly, Zn2 exhibits a similar coordination environment with Zn1 except that Zn2 weakly coordinates to O8B, so the coordination geometry of Zn2 calculated by SHAPE ver. 2.1 [52] is trigonal bipyramid compared with the tetrahedral of Zn1 (Table S3 in Supporting information). Moreover, the adjacent Zn^{II} ions are linked through two BBIP ligands to form a $[Zn_2(BBIP)_2]$ secondary building unit (SBU) (Fig. S1a in Supporting information), and the Zn···Zn distance is 9.258(8) Å. Furthermore, the SBUs are further connected by NDC^{2-} with μ_2-η^1:η^1 and μ_2-η^1:η^1:η^1 bridging modes (Fig. S1b in Supporting information) to form a two-dimensional (2D) framework (Fig. 1c). From the topological analysis, if Zn^{II} ions are considered as 3-connected nodes, $[Zn_2(BBIP)_2]$ secondary building units and NDC^{2-} ligands are considered as linkers, the whole 2D structure of **JXUST-5** could be simplified as a uninodal ***fes*** topology with a point symbol of $\{4.8^2\}$ rationalized by TOPOS 4.0 [53] (Fig. 1d). Furthermore, the 2D framework net could be extended through C–H···π interaction to form the three-dimensional supramolecular structure (Fig. 1e). The porosity of **JXUST-5** calculated by PLATON [54] is 2.3% of the unit cell (H_2O molecules were removed).

The solid-state emission spectra of **JXUST-5** as well as free BBIP and H_2NDC ligands were investigated at room temperature (Fig. S5 in Supporting information). The results indicated that there were emission peaks at 485 nm (λ_{ex} = 375 nm) for H_2NDC, and at 453 nm (λ_{ex} = 377 nm) for BBIP, respectively, which could be ascribed to the $\pi^*\rightarrow\pi$ and/or $\pi^*\rightarrow$n electron transfer [55]. Upon excitation at 344 nm, the emission band for **JXUST-5** was observed at 382 nm. Compared with the H_2NDC ligand, the emission peak of **JXUST-5** exhibits the obvious blue shift, which may be ascribed to the ligand-to-metal charge transfer [51]. Moreover, the luminescence properties of **JXUST-5** in EtOH solution were also carried out, which exhibits similar emission behavior to those in the solid state (Fig. S5 in Supporting information).

The fluorescence sensing experiments of **JXUST-5** toward metal ions were carried out with the EtOH suspension of **JXUST-5**. Because **JXUST-5** exhibits similar emission peak locations in EtOH solution compared with solid-state emission spectrum of **JXUST-5** (Fig. S5 in Supporting information), and the PXRD patterns of **JXUST-5** after immersing in EtOH solutions for 24 h, 3 days and 6 days were similar to that of as-synthesized **JXUST-5** (Fig. S4b in Supporting information), EtOH was chosen as the dispersion medium. The 1 mg finely ground samples were evenly immersed in 2 mL EtOH solutions containing 5 μL $M(NO_3)_x$ (0.2 mol/L, M^{x+}= K^+, Na^+, Li^+, Ag^+, Zn^{2+}, Mn^{2+}, Cd^{2+}, Mg^{2+}, Ca^{2+}, Ni^{2+}, Co^{2+}, Gd^{3+}, Eu^{3+}, Ga^{3+} and Al^{3+}) through ultrasonic agitation for 30 min to form steady suspensions. As presented in Fig. 2a, upon the addition of different metal ions, most of them showed a relatively weak influence on the luminescence intensity of **JXUST-5**. Notably, **JXUST-5** exhibited the excellent turn-on effect along with a relatively large red shift of 34 nm from 381 nm to 415 nm after the addition of Al^{3+}/Ga^{3+}. Interestingly, the suspensions of **JXUST-5** after the addition of Al^{3+}/Ga^{3+} showed the color change from light blue to blue, which could be directly observed with naked eyes under 365 nm UV lamp (Fig. 2b). Therefore, **JXUST-5** could be regarded as a promising fluorescent probe for detecting Al^{3+} and Ga^{3+} through fluorescence enhancement effect along with a relatively large red shift.

To further investigate the sensing sensitivity of **JXUST-5** toward Al^{3+} and Ga^{3+}, the fluorescence titration experiments were also carried out by gradually adding Al^{3+}/Ga^{3+} into the EtOH suspension of **JXUST-5**. As shown in Figs. 3a and c, the fluorescence intensity of **JXUST-5** gradually increased and obvious fluorescence red shift was observed upon the addition of Al^{3+}/Ga^{3+} concentration, which could be directly observed with naked eyes under 365 nm UV lamp (Figs. 4a and b). Furthermore, the good linear relationships in a low concentration range were observed in **JXUST-5** for sensing Al^{3+} and Ga^{3+} (Figs. 3b and d), and the K_{SV} values for Al^{3+} and Ga^{3+} are found to be 7.21 × 10^3 L/mol and 2.75 × 10^3 L/mol, respectively. In addition, the detection limits of **JXUST-5** toward Al^{3+} and Ga^{3+} are calculated to be 0.17 ppm (6.31 × 10^{-6} mol/L) and 0.69 ppm (9.93 × 10^{-6} mol/L), based on the well-established equation $3\sigma/k$ (k: the slope, σ: the standard error). As shown in Table S4 (Supporting information), MOF-based fluorescence sensors for the recognition of Al^{3+} with a turn-on mechanism in different medium solvents have been extensively studied, and the detection limit of **JXUST-5** toward Al^{3+} is comparable to those of previously reported turn-on luminescence sensors for Al^{3+} in EtOH solvent. More importantly, **JXUST-5** is the second example of turn-on MOF based fluorescent sensor toward Ga^{3+} [51] (Table S4 in Supporting information). Thus, **JXUST-5** could be regarded as a potential bifunctional fluorescence sensor toward Al^{3+} and Ga^{3+} with high sensitivity.

Considering the turn on sensing behavior of **JXUST-5** toward Al^{3+} and Ga^{3+} may be affected by other interfering metal ions,

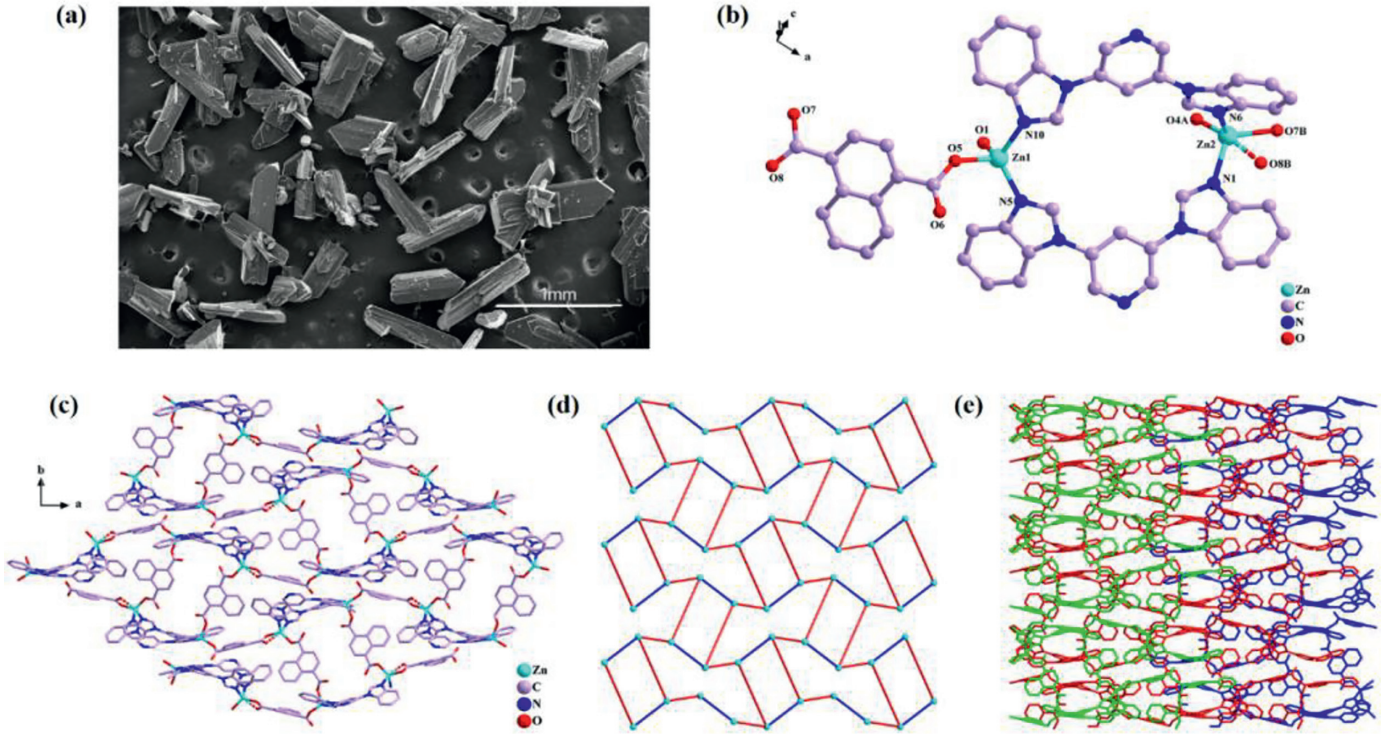

Fig. 1. (a) SEM image of **JXUST-5**. (b) The coordination environments of Zn^{II} ions in **JXUST-5** (H atoms omitted for clarity, symmetry codes: A: 1-*x*, 1-*y*, 1-*z*; B: 1 + *x*, 0.5-*y*, 0.5 + *z*). (c) The 2D network consisting of $[Zn_2(BBIP)_2]$ secondary building unit and NDC^{2-} in **JXUST-5**. (d) The topological structure of **JXUST-5** (Zn^{II} nodes, turquoise; $[Zn_2(BBIP)_2]$ secondary building unit linkers, bule; NDC^{2-} linkers, red). (e) The 3D supramolecular architecture of **JXUST-5**.

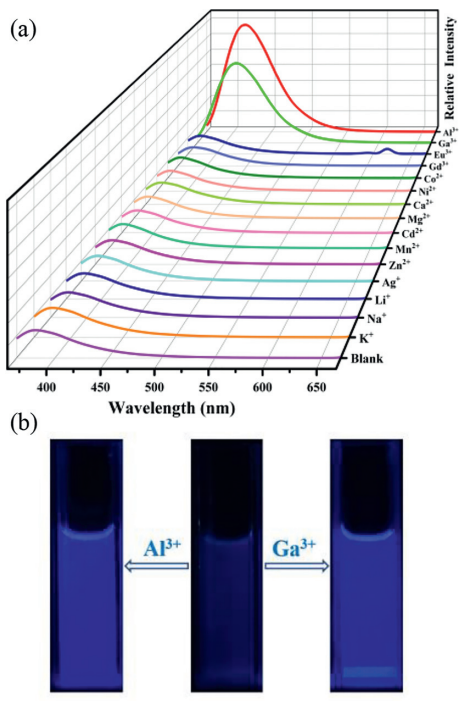

Fig. 2. (a) Emission spectra of **JXUST-5** dispersed in EtOH with the addition of different metal ions (5×10^{-4} mol/L), λ_{ex} = 344 nm. (b) Photos of the suspensions of **JXUST-5** before and after the addition of Al^{3+}/Ga^{3+} when excited with a hand-held 365 nm UV-lamp.

competitive experiments were further performed with the presence of 1 equiv. of other metal ions. Significantly, the turn-on effect as well as red-shift emission of **JXUST-5** toward Al^{3+} (Fig. S6a in Supporting information) and Ga^{3+} (Fig. S6b in Supporting information) still existed, verifying that **JXUST-5** has a high selectivity to detect Al^{3+} and Ga^{3+}.

The time-dependent fluorescence emission spectra were also performed. The fluorescence intensities and emission peak locations of the EtOH suspensions of **JXUST-5** with Al^{3+}/Ga^{3+} were continuously recorded (Figs. S7a and b in Supporting information). For Al^{3+} ion, an obvious fluorescence red shift was observed after 15 s. As time goes on, the fluorescence intensity slowly increases and reaches 4.3 times compared to the blank along with fluorescence red shift at 420 s. In terms of Ga^{3+} ion, after 15 s, an obvious fluorescence red shift was found, and at 420 s, the fluorescence intensity reaches about 3.1 times than that of the original one along with fluorescence red shift. The results further confirm the high sensitivity of **JXUST-5** toward Al^{3+} and Ga^{3+}.

The recycling capacity of **JXUST-5** as a luminescence probe was also studied in detail. The sample of **JXUST-5** was soaked in EtOH solutions containing Al^{3+}/Ga^{3+} for 30 min and washed by EtOH several times. Then the successive sensing experiments were carried out using the recovered solid. As depicted in Figs. S8a and b (Supporting information), the fluorescence intensities were essentially retained even after five recycling for detecting Al^{3+}/Ga^{3+}, and the framework was still maintained as confirmed by PXRD (Fig. S4c in Supporting information), demonstrating the outstanding stability of **JXUST-5** as fluorescent sensor toward Al^{3+} and Ga^{3+}during sensing process.

The possible turn-on sensing mechanism of **JXUST-5** toward Al^{3+} and Ga^{3+} has been further proposed. The PXRD patterns of **JXUST-5** immersed in EtOH solutions containing Al^{3+}/Ga^{3+} were

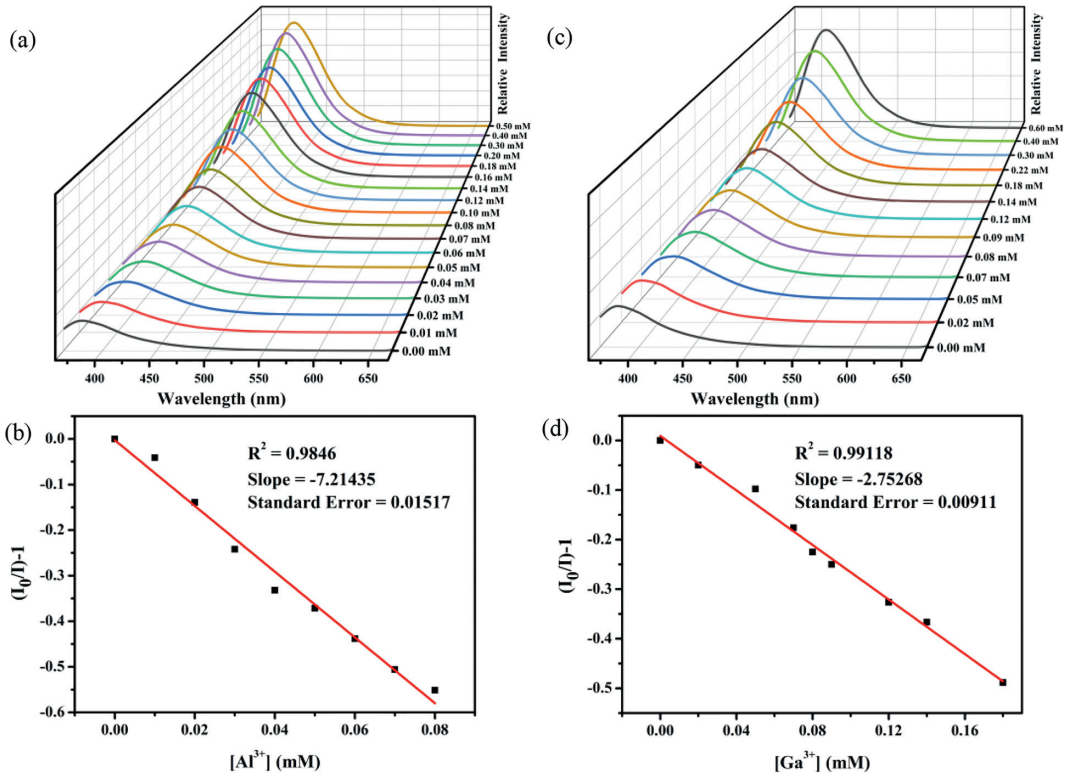

Fig. 3. Emission spectra of **JXUST-5** dispersed in EtOH suspension with various concentrations of (a) Al^{3+} ions and (c) Ga^{3+} ions, and the linear relationship in a low concentration range between the fluorescence intensity of **JXUST-5** and the concentration of (b) Al^{3+} ions and (d) Ga^{3+} ions.

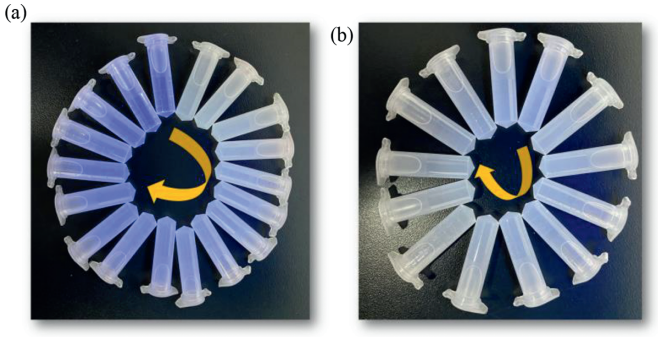

Fig. 4. Photographs of **JXUST-5** reacting with (a) 0–0.50 mmol/L (0, 0.01, 0.02, 0.03, 0.04, 0.05, 0.06, 0.07, 0.08, 0.10, 0.12, 0.14, 0.16, 0.18, 0.20, 0.30, 0.40, 0.50 mmol/L) Al^{3+} and (b) 0–0.60 mmol/L (0, 0.02, 0.05, 0.07, 0.08, 0.09, 0.12, 0.14, 0.18, 0.22, 0.30, 0.40, 0.60 mmol/L) Ga^{3+} under a hand-held 365 nm UV-lamp (the concentration increases with the direction of the yellow arrow).

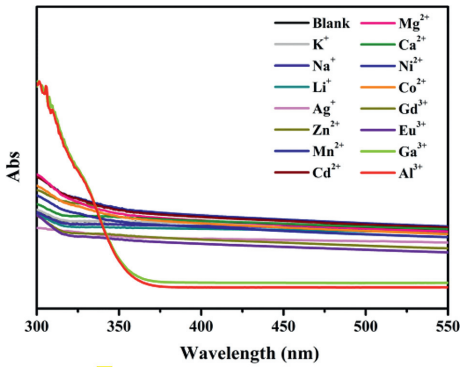

Fig. 5. UV–vis absorption spectra of **JXUST-5** upon the addition of various metal ions in EtOH solutions (5×10^{-4} mol/L).

similar to that of **JXUST-5** (Fig. S4a in Supporting information), which proved that the structure of **JXUST-5** is stable after the addition of Al^{3+}/Ga^{3+}. Moreover, it is also very diffcult for the neutral **JXUST-5** to capture Al^{3+}/Ga^{3+} through ion exchange. Hence, the sensing mechanism of **JXUST-5** toward Al^{3+} and Ga^{3+} might be owing to the interactions between the detected metal ions and the framework. Significantly, uncoordinated pyridine N atoms of BBIP ligand in **JXUST-5** may interact with detected metal ions. In order to explore the possible mechanism of the turn-on effect, the UV–vis absorption spectra of **JXUST-5** upon the addition of various metal ions were recorded. As shown in Fig. 5, the absorption intensity of **JXUST-5** shows a significant increase after adding Al^{3+}/Ga^{3+} in the range of 300–340 nm, while no obvious change was observed after the addition of various metal ions, which might be attributed to the interaction between the pyridine N atoms and Al^{3+}/Ga^{3+}. In order to eliminate the influence of metal ions itself on the UV–vis absorption intensity, the UV–vis absorption spectra of different metal ions in EtOH solutions have also been measured. As shown in Fig. S9 (Supporting information), no obvious absorbance in the range of 300–550 nm has been observed for metal ions, confirming that the absorbance enhancement of **JXUST-5** after adding Al^{3+}/Ga^{3+} is not from metal ions itself. Instead, the complexation of **JXUST-5** and Al^{3+}/Ga^{3+} causes the significant absorbance enhancement, thereby leading to the increase

of luminescent intensity. Therefore, the turn-on sensing mechanism of **JXUST-5** toward Al^{3+}/Ga^{3+} could be ascribed to the absorbance caused enhancement (ACE) [51], in which the absorbance of **JXUST-5** increases significantly after adding Al^{3+}/Ga^{3+}. In other words, the electrons of **JXUST-5**@Al^{3+}/Ga^{3+} complexation in the ground state could absorb more energy from the light source upon the addition of Al^{3+}/Ga^{3+}, and then transit to the excited state [51]. After a series of vibration relaxation, the excited electrons of **JXUST-5** return to the ground state, and simultaneously release energy in the form of luminescence [51]. In the emission process, the **JXUST-5**@Al^{3+}/Ga^{3+} complexation releases more energy than as-synthesized **JXUST-5**, and thus results in turn-on fluorescence [51]. In addition, the relationship between the concentration of Al^{3+}/Ga^{3+} and absorbance intensity of **JXUST-5** has been studied. As depicted in Figs. S10a and b (Supporting information), the absorbance intensity of **JXUST-5** gradually increased with increasing of the concentration of Al^{3+}/Ga^{3+}, which further proves the ACE mechanism. Finally, **JXUST-5** shows a remarkable fluorescence red shift upon the addition of Al^{3+}/Ga^{3+} (Fig. 2a). The red shift of the fluorescence emission indicates the possible existence of strong exciplex formation between **JXUST-5** and Al^{3+}/Ga^{3+} [56], which is further demonstrated by UV–Vis absorption spectra (Fig. 5). As a result, the most probable turn-on and red shift fluorescence mechanisms of **JXUST-5** toward Al^{3+} and Ga^{3+} could be interpreted as the ACE mechanism together with the formation of a strong exciplex between **JXUST-5** and Al^{3+}/Ga^{3+}.

In summary, a novel Zn^{II}-based MOF (**JXUST-5**) with ***fes*** topology has been synthesized by using mixed-ligand strategy. **JXUST-5** could selectively and sensitively recognize Al^{3+} and Ga^{3+} through fluorescence enhancement effect along with a relatively large red shift. The detection limits for Al^{3+} and Ga^{3+} are 0.17 and 0.69 ppm, respectively. Interestingly, the sensing process for both Al^{3+} and Ga^{3+} could be directly observed with naked eyes under 365 nm UV lamp. More importantly, **JXUST-5** could be recycled at least five times as a fluorescent sensor toward Al^{3+} and Ga^{3+}. The turn-on and fluorescence red shift mechanisms could be attributed to the ACE mechanism together with the formation of a strong exciplex between **JXUST-5** and Al^{3+}/Ga^{3+}. Notably, **JXUST-5** is the second case of turn-on MOF based fluorescent sensor toward Ga^{3+}. Unfortunately, if the solution contains Al^{3+} or Ga^{3+}, **JXUST-5** cannot give a discriminated signal. In the present work, we mainly focus on the construction of MOF-based fluorescence probes with a turn-on effect, and further study on the turn-on MOF sensors that identify specific metal ions is still on-going in our lab.

Declaration of competing interest

The authors declare that they have no known competing financial interests or personal relationships that could have appeared to influence the work reported in this paper.

Acknowledgments

This work was supported from the National Natural Science Foundation of China (Nos. 22061019, 21761012 and 21861018), the Natural Science Foundation of Jiangxi Province (Nos. 20192BAB203001, 20202ACBL213001, 20192ACBL20013 and 20182BCB22010), the Youth Jinggang Scholars Program in Jiangxi Province (No. QNJG2019053), and the Two Thousand Talents Program in Jiangxi Province (No. jxsq2019201068).

Supplementary materials

Supplementary material associated with this article can be found, in the online version, at doi:10.1016/j.cclet.2021.06.009.

References

[1] H.J. Jang, J.H. Kang, D. Yun, C. Kim, Photochem. Photobiol. Sci. 17 (2018) 1247–1255.
[2] Y.W. Wang, S.B. Liu, W.J. Ling, Y. Peng, Chem. Commun. 52 (2016) 827–830.
[3] V. Kumar, P. Kumar, S. Kumar, D. Singhal, R. Gupta, Inorg. Chem. 58 (2019) 10364–10376.
[4] Y.E. Yu, Y.H. Wang, H. Yan, et al., Inorg. Chem. 59 (2020) 3828–3837.
[5] X.M. Tian, S.L. Yao, C.Q. Qiu, et al., Inorg. Chem. 59 (2020) 2803–2810.
[6] M. Bonneau, C. Lavenn, P. Ginet, K.I. Otake, S. Kitagawa, Green Chem. 22 (2020) 718–724.
[7] J.Y. Zheng, X.L. Cui, Q.W. Yang, et al., Chem. Eng. J. 354 (2018) 1075–1082.
[8] Z.J. Chen, K. Adil, L.J. Weselinski, Y. Belmabkhout, M. Eddaoudi, J. Mater. Chem. A 3 (2015) 6276–6281.
[9] H.R. Tian, Z. Zhang, S.M. Liu, et al., J. Mater. Chem. A 8 (2020) 12398–12405.
[10] L. Mi, Y.D. Sun, L. Shi, T. Li, ACS Appl. Mater. Interfaces 12 (2020) 7879–7887.
[11] M.H. Li, J.X. Chen, W.W. Wu, Y.X. Fang, S.J. Dong, J. Am. Chem. Soc. 142 (2020) 15569–15574.
[12] X.B. Liu, T. Yue, K. Qi, et al., Chin. Chem. Lett. 31 (2020) 2189–2201.
[13] M.R. Cai, L.Y. Qin, L.T. You, et al., RSC Adv. 10 (2020) 36862–36872.
[14] Y.W. Li, Y. Song, W. Zhang, et al., J. Mater. Chem. B 8 (2020) 7382–7389.
[15] J. Gandara-Loe, B.E. Souza, A. Missyul, et al., ACS Appl. Mater. Interfaces 12 (2020) 30189–30197.
[16] S. Zhang, X. Pei, H.L. Gao, S. Chen, J. Wang, Chin. Chem. Lett. 31 (2020) 1060–1070.
[17] B. Yan, J. Mater. Chem. C 7 (2019) 8155–8175.
[18] K. Muller-Buschbaum, F. Beuerle, C. Feldmann, Micropor. Mesopor. Mater. 216 (2015) 171–199.
[19] J. He, J.L. Xu, J.C. Yin, N. Li, X.H. Bu, Sci. China Mater. 62 (2019) 1655–1678.
[20] Y.P. Li, H.R. Yang, Q. Zhao, et al., Inorg. Chem. 51 (2012) 9642–9648.
[21] X. Qian, S.Y. Deng, X. Chen, et al., Chin. Chem. Lett. 31 (2020) 2211–2214.
[22] N. Zhang, L.M. Yan, Y. Lu, et al., Chin. Chem. Lett. 31 (2020) 2071–2076.
[23] X. Wang, W.D. Fan, M. Zhang, et al., Chin. Chem. Lett. 30 (2019) 801–805.
[24] Z. Zhou, X.Q. Li, Y.P. Tang, et al., Chem. Eng. J. 351 (2018) 364–370.
[25] S. Biswas, A.K. Mondal, S. Konar, Inorg. Chem. 55 (2016) 2085–2090.
[26] R.M. Wen, S.D. Han, H. Wang, Y.H. Zhang, Chin. Chem. Lett. 25 (2014) 854–858.
[27] C. Cao, S.J. Liu, S.L. Yao, et al., Cryst. Growth Des. 17 (2017) 4757–4765.
[28] C.X. Yao, Y. Xu, Z.G. Xia, J. Mater. Chem. C 6 (2018) 4396–4399.
[29] P.C. Rao, S. Mandal, Inorg. Chem. 57 (2018) 11855–11858.
[30] H.L. Ma, L. Wang, J.H. Chen, et al., Dalton Trans. 46 (2017) 3526–3534.
[31] D.M. Chen, N.N. Zhang, C.S. Liu, M. Du, J. Mater. Chem. C 5 (2017) 2311–2317.
[32] G.X. Qiao, L. Liu, X.X. Hao, et al., Chem. Eng. J. 382 (2020) 122907.
[33] C. Zhan, S. Ou, C. Zou, M. Zhao, C.D. Wu, Anal. Chem. 86 (2014) 6648–6653.
[34] C.Y. Sun, X.L. Wang, C. Qin, et al., Chem. Eur. J. 19 (2013) 3639–3645.
[35] T. Wen, D.X. Zhang, Q.R. Ding, H.B. Zhang, J. Zhang, Inorg. Chem. Front. 1 (2014) 389–392.
[36] X.H. Zhou, H.H. Li, H.P. Xiao, et al., Dalton Trans. 42 (2013) 5718–5723.
[37] W. Yan, C.L. Zhang, S.G. Chen, L.J. Han, H.G. Zheng, ACS Appl. Mater. Interfaces 9 (2017) 1629–1634.
[38] M. Du, C.P. Li, C.S. Liu, S.M. Fang, Coord. Chem. Rev. 257 (2013) 1282–1305.
[39] A.J. Liu, F. Xu, S.D. Han, J. Pan, G.M. Wang, Cryst. Growth Des. 20 (2020) 7350–7355.
[40] S.D. Han, A.J. Liu, F. Xu, et al., Dalton Trans. 50 (2021) 546–552.
[41] Y.B. Wei, M.J. Wang, D. Luo, et al., Mater. Chem. Front. 5 (2021) 2416–2424.
[42] Y.N. Zeng, H.Q. Zheng, X.H. He, et al., Dalton Trans. 49 (2020) 9680–9687.
[43] S.L. Yao, X.M. Tian, L.Q. Li, et al., Chem. Asian J. 14 (2019) 3648–3654.
[44] L.L. Zhai, Y. Zhao, L. Luo, et al., Microporous Mesoporous Mater. 187 (2014) 86–93.
[45] X.L. Wang, L.L. Hou, J.W. Zhang, C.H. Gong, G.C. Liu, Inorg. Chim. Acta 405 (2013) 58–64.
[46] S.L. Yao, S.J. Liu, X.M. Tian, et al., Inorg. Chem. 58 (2019) 3578–3581.
[47] T.F. Xia, L.C. Jiang, J. Zhang, et al., Micropor. Mesopor. Mater. 305 (2020) 110396.
[48] H. Li, D.L. Li, B.W. Qin, et al., Dyes Pigm. 178 (2020) 108359.
[49] Q. Zhang, M. Lei, H. Yan, J. Wang, Y. Shi, Inorg. Chem. 56 (2017) 7610–7614.
[50] Y.Q. Chen, Y. Tian, S.L. Yao, et al., Chem. Asian J. 14 (2019) 4420–4428.
[51] M. Wang, L. Guo, D.P. Cao, Sens. Actuator. B: Chem. 256 (2018) 839–845.
[52] M. Llunell, D. Casanova, J. Cirera, P. Alemany, S. Alvarez, SHAPE, Version 2.1, Universitat de Barcelona, Barcelona, Spain, 2013.

[53] V.A. Blatovd, A.P. Shevchenko, TOPOS, ver. 4.0 Professional (Beta Evaluation), Samara State University, Samara, Russia, 2006.
[54] A.L. Spek, Acta Cryst. C 71 (2015) 9–18.
[55] Y. Wang, P. Xu, Q. Xie, et al., Chem. Eur. J. 22 (2016) 10459–10474.
[56] S. Pramanik, Z.C. Hu, X. Zhang, et al., Chem. Eur. J. 19 (2013) 15964–15971.